International Journal of Applied Engineering Research ISSN 0973-4562 Volume 12, Number 15 (2017) pp. 4847-4853

An Efficient Control of Induction Generator based Variable Speed Wind Power Plant with Power Optimization Capability

[1]Neha Gupta and [2]Yaduvir Singh

Department of Electrical Engineering, School of Engineering,
Harcourt Butler Technical University, Kanpur (U.P.), India.

[1]Orcid Id: 0000-0003-1512-309X

Abstract
In this work we have presented extremum seeking (ES) control for maximum power extraction in variable speed fixed pitch (VSFP) grid connected wind power plant. For modeling of wind power plant we have considered squirrel cage induction generator (SCIG) as wind generator (WG) and matrix converter (MC) as power electronic interface between WG and grid. Matrix converter facilitates the mechanism of ES scheme. Unlike other MPPT techniques, ES is a non model based MPPT algorithm. In this paper sinusoidal signal has been used as a search disturbance signal. The performance of the ES algorithm has been checked for different wind velocities. In the latter section of this paper, we have designed a non-linear controller based on to prevent the magnetic saturation of induction generator. Also we made a comparison between the results obtained with and without the non-linear controller.

Keywords: Wind generator, Extremum seeking, MPPT, stability, SCIG, Controller

INTRODUCTION

In last few decades due to environmental issues, researchers are more inclined towards the non conventional and clean ways of energy production. Of various non conventional energy resources, the wind energy is considered to be most promising source of energy because of its abundance cleanliness, free availability and technical maturity [1-4]. The popular structures in wind power plant include squirrel cage induction generator (SCIG) based wind power plant, doubly fed induction generator (DFIG) based wind power plant and permanent magnet synchronous generator (PMSG) based wind power plant [5-7]. All these systems offer good efficiency, lesser aerodynamic load and easy regulation of active and reactive powers. The SCIG provides flexibility under varying wind speed due to its asynchronous operation, so here in this work we have used SCIG. SCIG also offers economy, simplicity and robustness in structure against disturbance and vibration.

To extract maximum power from a wind power plant at varying wind speeds, an MPPT design is required which alters the shaft speed of turbine using varying wind speed method , which intern will alter the power output, since the power output is proportional to the turbine angular velocity. This change in shaft speed is done through a power electronic interface between WG and grid, for which we have to control the switching of power electronic converter. Here in this paper we have used matrix (ac-dc-ac) converter instead of conventional rectifier inverter pair. The advantage of using matrix converter is that it allows flow of power in both the directions and input power factor is also controllable. In addition it has no energy storage components [8-9]. By switching of matrix converter, we alter the stator electrical frequency, which leads to the change in turbine shaft speed and drives SCIG to its maximum power point (MPP). The techniques available until now, which include perturb and observe (P & O) methods, fuzzy and neural network based techniques, are highly model dependent. The main disadvantage of model based optimization techniques is that every time we use a new model, new controller has to be designed for MPPT, which is a tedious task [10]. In this work extremum seeking scheme has been used, which is a model independent algorithm. Also it offers easy tenability, design simplicity and performance stoutness [3, 7, 15].

WIND POWER PLANT

A general block diagram of wind power plant contains wind turbine, WG, power electronic interface to achieve MPPT at varying wind speeds and load. Here in this paper, we are using matrix converter as power electronic interface and our wind generator is SCIG. Since we are modeling grid connected wind power plant, we have utility grid in place of load. In order to know the dynamics of wind turbine, we also need to model the wind turbine aerodynamics. The block diagram considered in this paper is shown in Figure.1.

The power captured by the VSWT is expressed in terms power coefficientC_p, which is a dimensionless quantity.

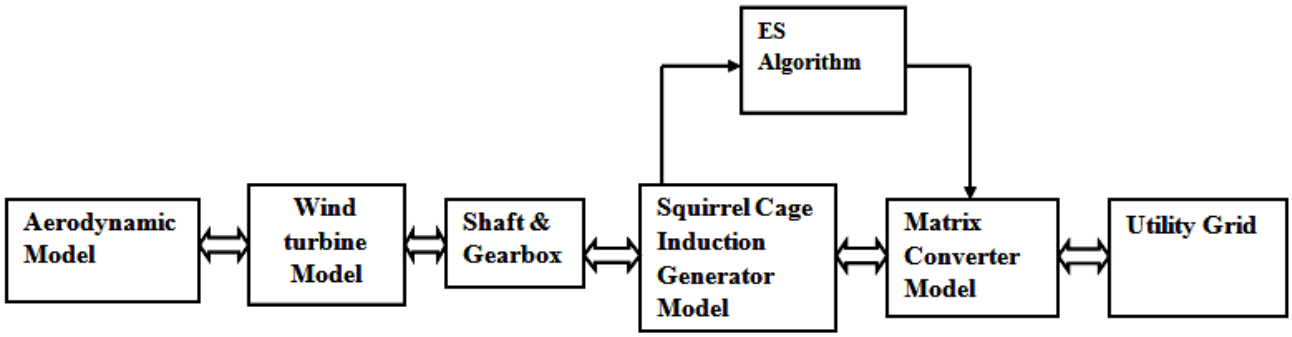

Figure 1. Block diagram of Wind power plant model under study.

C_P is a measure of the ratio of the rotor power to the wind power as indicated by (1):

$$P_T = \frac{1}{2}\rho A_r C_P(\lambda,\beta)V_\omega^3 \quad (1)$$

Maximum torque extracted from the turbine rotor can be given as

$$T_T = \frac{1}{2\omega_t}\rho A_r C_P(\lambda,\beta)V_\omega^3 \quad (2)$$

Where TSR (tip speed ratio) is defined as

$$\lambda = \frac{blade\ tip\ speed}{wind\ speed} = \frac{\omega_t \times R}{V_\omega}$$

V_ω = speed of wind in m/s
A = swept area of wind turbine blade
ω_t = turbine angular speed.
λ = TSR and β = Pitch angle of rotor blade

C_p is related to λ, and β. Here, we have considered C_p curve to be [2]:

$$C_p = 0.73\ \frac{151\frac{V_w}{R\omega_t} - 13.635}{\exp\left(\frac{V_w}{R\omega_t} - 0.003\right)} \quad (3)$$

From figure.2, it is clear that C_p remains at the same level, if the turbine speed is varied with each change in wind speed.

Figure.3 shows the change in turbine power with each change in angular velocity for different wind speeds.

Figure.4. shows that if we join the points of at which the turbine power is maximum, a curve of third-order defining the maximum power attained by the wind turbine is obtained.

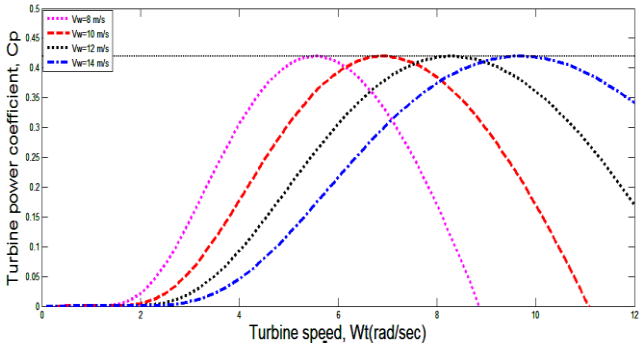

Figure 2. Power coefficient vs. turbine speed curve.

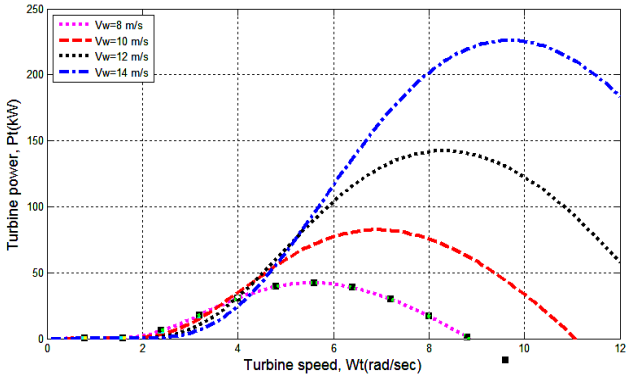

Figure 3. Turbine power vs. turbine speed curve.

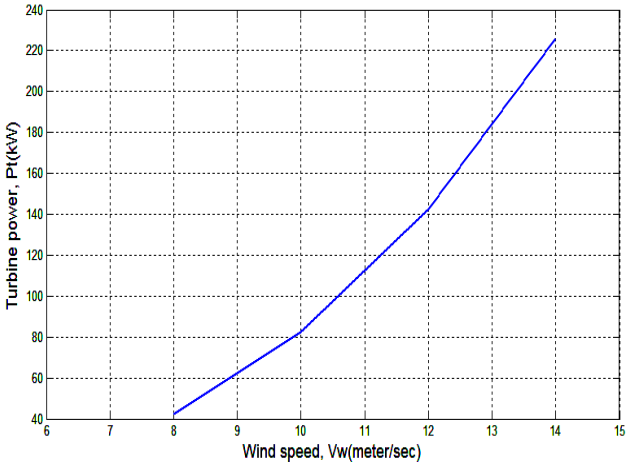

Figure 4. Turbine speed vs. wind speed curve.

The overall model for wind energy conversion system may be given by following eight nonlinear equations, which includes the state-equation of the mechanical shaft, electrical generator, and the matrix converter [11-14].

$$\frac{d}{dt}i_\alpha = -a_0 i_\alpha + a_1\lambda_\alpha + a_2\omega_r\lambda_\beta + \frac{\cos\theta_0}{\sigma L_s}V_{0m} \quad (4)$$

$$\frac{d}{dt}i_\beta = -a_0 i_\beta + a_1\lambda_\beta + a_1\omega_r\lambda_\alpha + \frac{\sin\theta_0}{\sigma L_s}V_{0m} \quad (5)$$

$$\frac{d}{dt}\lambda_\alpha = a_3 i_\alpha - a_4\lambda_\alpha - \omega_r\lambda_\beta \quad (6)$$

$$\frac{d}{dt}\lambda_\beta = a_3 i_\beta - a_4\lambda_\beta + \omega_r\lambda_\alpha \quad (7)$$

$$\frac{d}{dt}\theta_0 = \omega_0 \quad (8)$$

$$\frac{d}{dt}\omega_r = \frac{3p^2 L_m}{2L_r J}\left(i_\beta\lambda_\alpha - i_\alpha\lambda_\beta\right) - \frac{pK_s}{nJ}\tilde{\theta} - \frac{pB}{nJ}\left(\omega_t - \frac{\omega_r}{pn}\right) \quad (9)$$

$$\frac{d}{dt}\tilde{\theta} = \omega_t - \frac{\omega_r}{pn} \quad (10)$$

$$\frac{d}{dt}\omega_t = -\frac{P_t(V_w,\omega_t)}{J_t\omega_t} - \frac{K_s}{J_t}\tilde{\theta} - \frac{B}{J_t}\left(\omega_t - \frac{\omega_r}{pn}\right) \quad (11)$$

EXTREMUM SEEKING FOR MAXIMUM POWER EXTRACTION IN WIND POWER PLANT

A typical power curve of a WECS as shown in Figure.5 can be divided into four major regions. The first region contains the velocities below which turbine is not able to generate any power due to insufficient wind. The second region contains the wind velocities from where the generation starts to the velocity up till which the power linearly increases with increase in wind velocity. This region is known as sub-rated power region. This is the region where MPPT schemes are applied to capture maximum power; hence power output is limited by wind turbine. The fourth region contains the velocities of wind which are much stronger and may cause damage to wind turbine, hence in this region, the turbine is shut down [18].

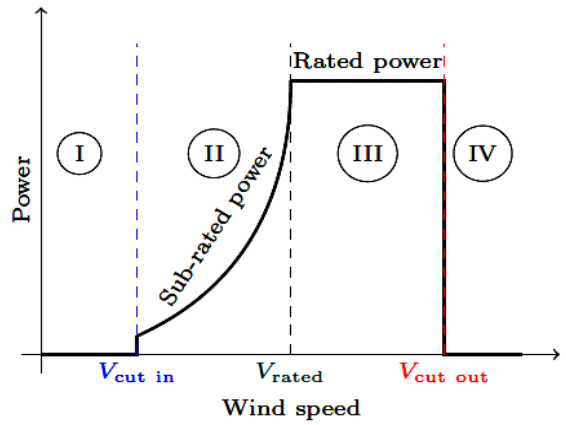

Figure 5. Wind speed vs. power curve showing four operating regions [18].

Now we present the extremum seeking technique for WECS, which is a real time optimization techniques and unlike conventional MPPT algorithms it does not require system modeling and identification. For simulation purpose the models of C_p and turbine power are given eq. (3) and (4). Here it is assumed that we can measure & manipulate turbine power through MC. As, the turbine power map has one MPP under any wind speed, we make the following assumption

For $V_{cut\ in} < V_w < V_{rated}$ (Figure.5).

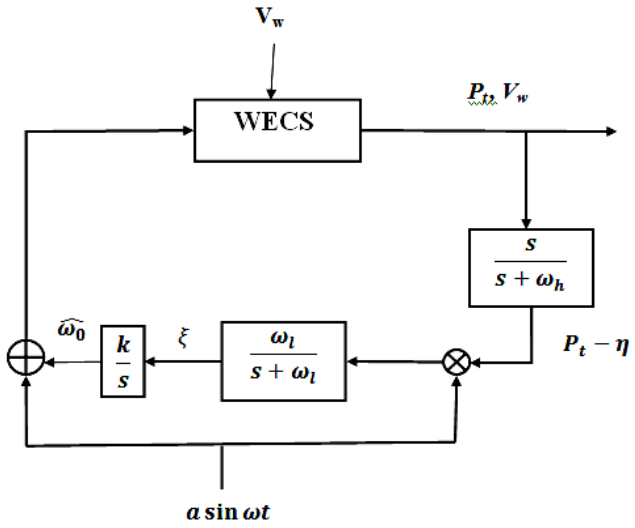

Figure 6. Extremum seeking scheme for extraction of maximum power in wind power plant (without inner loop).

$$\frac{\partial P_t(V_w,\omega_t)}{\partial\omega_t}(\omega_t^*) = 0 \quad (12)$$

$$\frac{\partial^2 P_t(V_w,\omega_t)}{\partial^2\omega_t}(\omega_t^*) < 0 \quad (13)$$

If, we carefully study the torque speed characteristics of an induction machine, it is observed that this curve is very sharp near the synchronous speed (stator electrical frequency), ω_0. At this point the rotor electrical speed ω_r and synchronous speed ω_0 will be nearly equal. This indicates that if we change the stator electrical frequency, the electrical rotor speed will change, which intern will change the turbine speed ω_t[19].Thus by varying $\omega_0$through MC, we may change turbine speed ω_t to track MPPT. Our ES scheme works on the same line.

CONTROL STRATEGY OF NON-LINEAR STATE FEEDBACK CONTROLLER

In case of flux transient the dynamics of system are non linear and coupled. So we have used a non-linear controller based on field oriented control and feedback linearization to

prevent magnetic saturation of induction generator and improve the performance of the system [14].

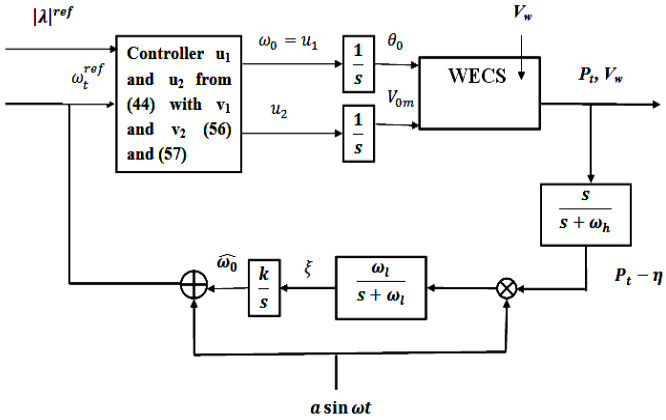

Figure 7. Extremum seeking for MPPT in WECS with inner loop.

$$y_1 = \Psi_1(x) = x_9 \tag{14}$$

$$y_2 = \mathcal{L}_f\Psi_1(x) = -a_9\left(x_9 - \frac{x_7}{pn}\right) - a_8x_8 - \frac{T_t}{J_t} \tag{15}$$

$$y_3 = \mathcal{L}_f^2\Psi_1(x) = b_0\xi_q + b_1\mathcal{L}_f\Psi_1(x) + b_2x_8 + b_3\frac{T_t}{J_t} - \tag{16}$$

$$y_4 = \mathcal{L}_f^3\Psi_1(x) = b_4\mathcal{L}_f^2\Psi_1(x) + b_5\mathcal{L}_f\Psi_1(x) + b_6x_8 - \frac{b_0}{\sigma L_s}x_6\lambda_q - x_7\left(b_7\Psi_2(x) + b_8\mathcal{L}_f\Psi_2(x)\right) + b_9\frac{T_t}{J_t} \tag{17}$$

$$\eta_1 = \Psi_2(x) = x_3^2 + x_4^2 \tag{18}$$

$$\eta_2 = \mathcal{L}_f\Psi_2(x) = 2a_3\xi_d - 2a_4\Psi_2(x)) \tag{19}$$

$$\eta_3 = \mathcal{L}_f^2\Psi_2(x) = b_{12}\Psi_2(x) + b_{11}\mathcal{L}_f\Psi_2(x) + b_{13}x_7\left(\mathcal{L}_f^2\Psi_2(x) - b_1\mathcal{L}_f\Psi_2(x) - b_2x_8 + b_3\frac{T_t}{J_t} + \frac{\dot{T}_t}{J_t}\right) + 2a_3^2i_s + \frac{2a_3}{\sigma L_s}x_6 \tag{20}$$

$$\Delta = x_8 \tag{21}$$

$$\varphi = \arctan\left(\frac{x_4}{x_3}\right) \tag{22}$$

where $\xi_d = x_1x_3 + x_2x_4$, $\xi_q = x_2x_3 - x_1x_4$, $i_s = i_\alpha^2 + i_\beta^2$ and

$$\begin{bmatrix}\lambda_d\\ \lambda_q\end{bmatrix} = \begin{bmatrix}\cos x_5 & \sin x_5\\ -\sin x_5 & \cos x_5\end{bmatrix}\begin{bmatrix}x_3\\ x_4\end{bmatrix} \tag{23}$$

The inverse transformation of (14)-(22)

$$\begin{bmatrix}x_1\\ x_2\end{bmatrix} = \frac{1}{\sqrt{\eta_1}}\begin{bmatrix}\cos\varphi & -\sin\varphi\\ \sin\varphi & \cos\varphi\end{bmatrix}\begin{bmatrix}\Psi_d\\ \Psi_q\end{bmatrix} \tag{24}$$

$$x_3 = \sqrt{\eta_1}\cos\varphi \tag{25}$$

$$x_4 = \sqrt{\eta_1}\sin\varphi \tag{26}$$

$$x_5 = \arctan\left(\frac{\Upsilon_\beta}{\Upsilon_\alpha}\right) \tag{27}$$

$$x_6 = \sqrt{\Upsilon_\alpha^2 + \Upsilon_\beta^2} \tag{28}$$

$$x_7 = pn\left(y_1 + \frac{y_2}{a_9} + \frac{a_8}{a_9}\Delta + \frac{T_t}{a_9J_t}\right) \tag{29}$$

$$x_8 = \Delta \tag{30}$$

$$x_9 = y_1 \tag{31}$$

$$\Psi_d = \frac{\eta_2 + 2a_4\eta_1}{2a_3} \tag{32}$$

$$\Psi_q = \frac{1}{b_0}\left(y_3 - b_1y_2 - b_2\Delta - b_3\frac{T_t}{J_t} + \frac{\dot{T}_t}{J_t}\right) \tag{33}$$

With

$$\Phi_d\frac{\sigma L_s}{2a_3}(\eta_3 + 2a_4\eta_2 - 2a_1a_3\eta_1 - 2a_3^2i_s) \tag{34}$$

$$\Phi_q = \frac{\sigma L_s}{b_0}\left(y_4 - b_1y_3 + \frac{a_8^2}{a_9^2}y_2 + \frac{a_8^2}{a_9^2}\Delta + b_0(a_0 + a_4)\Psi_q + b_0x_7\left(\Psi_q + a_2\eta_1\right) + \frac{a_8^2}{a_9^2}\frac{T_t}{J_t} - b_3\frac{T_t}{J_t} + \frac{\dot{T}_t}{J_t}\right) \tag{35}$$

Assigning a new variable for each differential, we obtain:

$$\dot{y}_1 = y_2 \tag{36}$$

$$\dot{y}_2 = y_3 \tag{37}$$

$$\dot{y}_3 = y_4 \tag{38}$$

$$\dot{y}_4 = G_1 + \frac{b_0\lambda_d}{\sigma L_s}x_6u_1 - \frac{b_0\lambda_q}{\sigma L_s}u_2 \tag{39}$$

$$\dot{\eta}_1 = \eta_2 \tag{40}$$

$$\dot{\eta}_2 = \eta_3 \tag{41}$$

$$\dot{\eta}_3 = G_2 + \frac{2a_3\lambda_q}{\sigma L_s}x_6u_1 - \frac{2a_3\lambda_d}{\sigma L_s}u_2 \tag{42}$$

With

$$\begin{bmatrix}i_d\\ i_q\end{bmatrix} = \begin{bmatrix}\cos x_5 & \sin x_5\\ -\sin x_5 & \cos x_5\end{bmatrix}\begin{bmatrix}x_1\\ x_2\end{bmatrix} \tag{43}$$

Defining the signal as follows

$$\begin{bmatrix}x_6u_1\\ u_2\end{bmatrix} = \frac{\sigma L_s}{\sqrt{\eta_1}}\begin{bmatrix}\cos(\varphi - \theta_0) & -\sin(\varphi - \theta_0)\\ \sin(\varphi - \theta_0) & \cos(\varphi - \theta_0)\end{bmatrix}\begin{bmatrix}\frac{v_1 - G_1}{b_0}\\ \frac{v_2 - G_2}{2a_3}\end{bmatrix} \tag{44}$$

Assigning new set of variables again, we get:

$$z = \left[y_1 - \omega_t^{ref}, y_2, y_3, y_4\right]^T \tag{45}$$

$$\zeta = [\eta_1 - (|\lambda|^{ref})^2, \eta_2, \eta_3]^T \tag{46}$$

We obtain

$$\dot{z}_1 = z_2 \quad (47)$$

$$\dot{z}_2 = z_3 \quad (48)$$

$$\dot{z}_3 = z_4 \quad (49)$$

$$\dot{z}_4 = v_1 \quad (50)$$

$$\dot{\zeta}_1 = \zeta_2 \quad (51)$$

$$\dot{\zeta}_2 = \zeta_3 \quad (52)$$

$$\dot{\zeta}_3 = v_2 \quad (53)$$

$$\dot{\Delta} = -\frac{z_2}{a_9} - \frac{a_8}{a_9}\Delta - \frac{T_t}{a_9 J_t} \quad (54)$$

$$\dot{\varphi} = \omega_r + \frac{a_3}{b_0\eta_1}\left(z_3 - b_1 z_2 - b_2\Delta - b_3\frac{T_t}{J_t} + \frac{\dot{T}_t}{J_t}\right) \quad (55)$$

Linear state feedback

$$v_1 = -k_1' z_1 - k_2' z_2 - k_3' z_3 - k_4' z_4 \quad (56)$$

$$v_2 = -k_1'' \zeta_1 - k_2'' \zeta_2 - k_3'' \zeta_3 \quad (57)$$

Where $b_0 = \frac{a_5 a_9}{pn}$, $\boldsymbol{b_1} = a_8/a_9 + a_7/pn - a_9$, $\boldsymbol{b_2} = a_8^2/a_9$, $\boldsymbol{b_3} = a_8/a_9 + a_7/pn$,

$\boldsymbol{b_4} = b_1 - a_0 - a_4$, $\boldsymbol{b_5} = a_0 b_1 + a_4 b_1 - b_2/a_9$, $\boldsymbol{b_6} = a_0 b_2 + a_4 b_2 - a_8 b_2/a_9$, $\boldsymbol{b_7} = a_2 b_0 + + a_4 b_0/a_3$, $\boldsymbol{b_8} = b_0/2a_3$, $\boldsymbol{b_9} = a_0 b_3 + a_4 b_3 - b_2/a_9$, $\boldsymbol{b_{10}} = b_3 - a_0 - a_4$, $\boldsymbol{b_{11}} = a_0 + 3a_4$, $\boldsymbol{b_{12}} = 2a_1 a_3 - 2a_0 a_4 - 2a_4^2$, $\boldsymbol{b_{13}} = 2a_3/b_0$

SIMULATION RESULTS

The proposed extremum seeking feedback scheme for MPPT in WECS has been evaluated by testing it for different disturbances i.e. variation of wind speeds in sub-rated power region using MATLAB m-file. The results are presented below. To check the performance of inner loop we applied a wind velocity 0f 10 m/s for 30s and then changed it suddenly to 11 m/s. Figure.8. shows the responses of the proposed WECS incorporating the ES based control of SCIG with and without inner loop control, for sudden wind speed variation. It is seen clear from Figure. 9 & 10 that without inner loop the power coefficient greatly varies with change in wind speed but with inner loop the variation of Cp with change in speed is very less, while with increase in wind speed the power level increases.

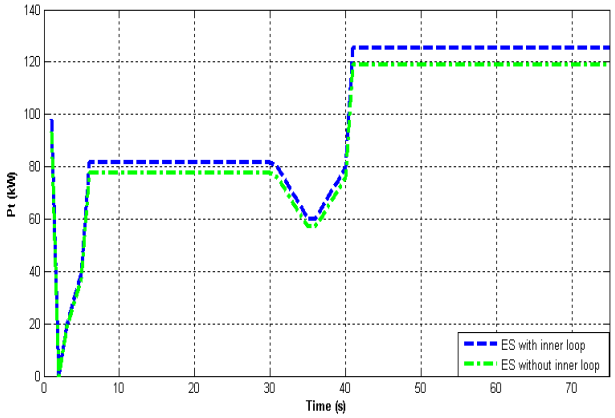

Figure 8. MPPT without inner loop, (dotted green line), MPPT with inner loop, (dotted blue line)

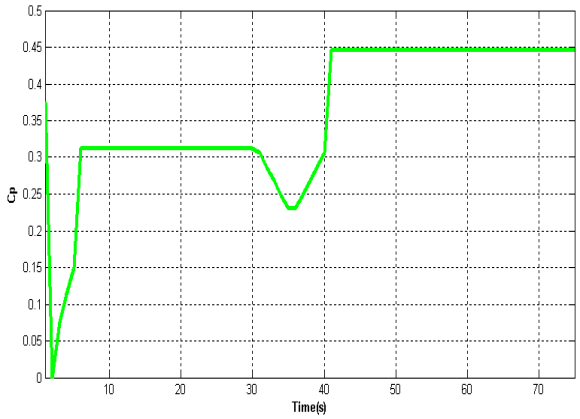

Figure 9. Power coefficient variation with inner loop control

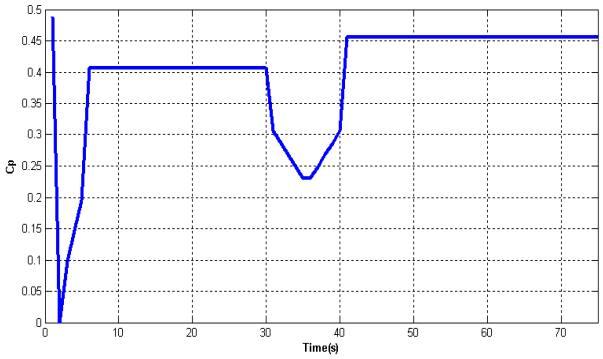

Figure 10. Power coefficient variation with inner loop control

CONCLUSION

We have presented extremum seeking feedback algorithm for maximum power extraction in wind power plant. ES scheme estimates the stator electrical frequency to steer the wind turbine to its maximum power point. We have checked the performance of this control system for sudden

wind variation and found that as soon as we change the wind velocity the ES scheme steers the wind turbine to its corresponding MPP. Further we have applied a non linear controller to the same system, which is based on field oriented control and feedback linearization. The non linear controller is used for the transient performance improvement of the proposed wind power plant. The advantageous feature of this work is that it is independent of the knowledge of wind speed, turbine or generator parameters. So, once we have designed the controller, it can be applied to any WECS model. We have also done the stability analysis of Es scheme for WECS and found that it successfully converges at MPP.

REFERENCES

[1] Jiawei Chen, Jiechen, chunying Gong, "On optimizing the transient load of variable speed wind energy conversion system during MPP tracking process", *IEEE transaction on Industrial Electronics, Vol-61, Issue-9, 2013,pp.-4698-4706.*

[2] S. M. Barakati, "Modeling and controller design of a wind energy conversion system including a matrix converter," Ph.D. dissertation, Dept. Electr. Comput. Eng., University of Waterloo, Waterloo, ON, Canada, 2008.

[3] X. She, A. Q. Huang, F. Wang, and R. Burgos, "Wind energy system with integrated functions of active power transfer, reactive power compensation, and voltage conversion," *IEEE Trans. Ind. Electron.*, vol. 60, no. 10, pp. 4512–4524, Oct. 2013.

[4] L. Barote, C. Marinescu, and M. N. Cirstea, "Control structure for single-phase stand-alone wind-based energy sources," *IEEE Trans. Ind. Electron.*, vol. 60, no. 2, pp. 764–772, Feb. 2013.

[5] N. Wang, K. E. Johnson, and A. D. Wright, "Comparison of strategies for enhancing energy capture and reducing loads using LIDAR and feed forward control," *IEEE Trans. Control Syst. Technol.*, vol. 21, no. 4, pp. 1129–1142, Jul. 2013.

[6] L. Shuhui, T. A. Haskew, K. A. Williams, and P. R. Swatloski, "Control of DFIG wind turbines with direct-current vector control configuration," *IEEE Trans. Sustain. Energy*, vol. 3, no. 1, pp. 1–11, Jan. 2012.

[7] M. F. M. Arani and E. F. EI-Saadany, "Implementing virtual inertia in DFIG-based wind power generation," *IEEE Trans. Power Syst.*, vol. 28, no. 2, pp. 1373–1384, May 2013.

[8] T. H. Nguyen and D.-C. Lee, "Advanced fault ride-through technique for PMSG wind turbine systems using line-side converter as STACOM," *IEEE Trans. Ind. Electron.*, vol. 60, no. 7, pp. 2842–2850, Jul. 2013.

[9] S. Zhang, K. J. Tseng, and T. D. Nguyen, "Modeling of AC-AC matrix converter for wind energy conversion system," in *Proc. IEEE Conf. Ind. Electron. Appl.*, May 2009, pp. 184–191.

[10] A. I. Bratcu, E. C. Iulian Munteanu, and S. Epure, "Energetic optimization of variable speed wind energy conversion systems by extremum seeking control," in *The International Conference on "Computer as a Tool"*, 2007.

[11] P. C. Krause, O. Wasynczuk, and S. D. Sudhoff, *Analysis of Electric Machinery and Drive Systems*. New York, NY, USA: Wiley, 2002.

[12] A. D. Luca and G. Ulivi, "Dynamic decoupling of voltage frequency controlled induction motors," in *Proc. 8th Int. Conf Anal. Optim. Syst.*, 1988, pp. 127–137.

[13] A. D. Luca and G. Ulivi, "Design of exact nonlinear controller for induction motors," *IEEE Trans. Autom. Control*, vol. 34, no. 12, pp. 1304–1307, Dec. 1989.

[14] R. Marino, S. Peresada, and P. Valigi, "Adaptive input-otput linearizing control of induction motors," *IEEE Trans. Autom. Control*, vol. 38, no. 2, pp. 208–221, Feb. 1993.

[15] M. Komatsu, H. Miyamoto, H. Ohmori, and A. Sano, "Output maximization control of wind turbine based on extremum control strategy," in *Proc. of American Control Conference*, 2001.

[16] V. Kumar, R. R. Joshi, and R. C. Bansal, "Optimal control of matrixconverter- based WECS for performance enhancement and efficiency optimization," *IEEE Transaction on Energy Conversion*, vol. 24, pp. 264–273, 2009.

[17] T. Pan, Z. Ji, and Z. Jiang, "Maximum power point tracking of wind energy conversion systems based on sliding mode extremum seeking control," in *Proc. IEEE Energy 2030 Conference*, 2008.

[18] A. Ghaffari, M. Krstic, S. Seshagiri, "Power optimization and control in wind energy conversion system using extremum seeking", *IEEE Transaction on Control System Technology, Vol-22, Issue 5,2014.*

[19] M. Krsti´c and H.-H. Wang, "Stability of extremum seeking feedback for general nonlinear dynamic systems," *Automatica*, vol. 36, no. 4, pp. 595–601, 2000.

[20] Khalil, H.K. (1996). *Nonlinear systems* (2nd ed.). Englewood Cli!s, NJ: Prentice Hall.

APPENDIX

TABLE-I CONSTANT PARAMETERS

$\boldsymbol{a_0}$	$a_2 a_3 + \frac{R_s}{\sigma L_s}$,
$\boldsymbol{a_1}$	$a_2 a_4$
$\boldsymbol{a_2}$	$\frac{L_m}{\sigma L_s L_r}$
$\boldsymbol{a_3}$	$\frac{L_m R_r}{L_r}$
$\boldsymbol{a_4}$	$\frac{R_r}{L_r}$
$\boldsymbol{a_5}$	$3p^2 L_m / 2JL_r$
$\boldsymbol{a_6}$	pK_s/Jn
$\boldsymbol{a_7}$	pB/Jn
$\boldsymbol{a_8}$	K_s/J_t
$\boldsymbol{a_9}$	B/J_t